Dynamic Study of the Oxidation State of Copper in the Course of Carbon Monoxide Oxidation over Powdered CuO and Cu_2O

K. Nagase, Y. Zheng, Y. Kodama, and J. Kakuta

Department of Chemistry, Graduate School of Science, Tohoku University, Sendai 980-8578, Japan
E-mail: naga@mail.cc.tohoku.ac.jp

Variations in the oxidation state of copper during CO catalytic oxidation over powdered CuO and Cu_2O in a gas mixture of 5% CO/He and air (O_2) were investigated by means of an appropriate combination of evolved gas analysis, thermogravimetry, XRD, and FT-IR in the temperature range of RT to 350°C, and these variations were compared with those observed when both oxides were individually reacted with CO (5% CO/He) and with air. The catalytic rate over CuO was found to almost agree with the bulk reduction rate of $CuO \rightarrow Cu$, while the catalytic rate over Cu_2O agreed with the bulk reduction rate of $CuO^* \rightarrow Cu_2O$, where CuO^* denotes a metastable divalent copper oxide produced in the oxidizing process of Cu_2O. Adsorption of O_2^- and/or O^- was characteristic of CuO^*, in contrast with that of O_2 and/or O of CuO. Variations in copper valence of a catalyst surface were concluded to be $II \leftrightarrows I$ for CuO and $I \rightarrow II \leftrightarrows I$ for Cu_2O, and the catalytic rates were determined by the reducing processes of CuO and CuO^* given by $O_{lc}^{2-} + O_{2\,ads}$ (or O_{ads}) $+ CO_{ads} \rightarrow CO_2 + O_{2\,ads}$ (or O_{ads}) $+ 2e^-$ followed by copper valence changes of $II \rightarrow 0$ and $O_{lc}^{2-} + O_{2\,ads}^-$ (or O_{ads}^-) $+ 1/2CO \rightarrow 1/2O_{lc}^{2-} + O_{2\,ads}^-$ (or O_{ads}^-) $+ 1/2CO_2 + e^-$ followed by that of $II \rightarrow I$, where O_{lc}^{2-} denotes lattice oxygen. © 1999 Academic Press

INTRODUCTION

Copper is one of the most widely used catalysts because of its high activity and selectivity as an oxidation/reduction catalyst. The oxidation state of copper changes thermodynamically between CuO, Cu_2O, and Cu as a function of temperature and oxygen partial pressure (1). The differences in oxygen defects, oxygen holes, and oxygen adsorption species in these oxidation states are thought to be the reason for the high activity or selectivity of copper catalysts. Most reactions are thought to proceed through a redox cycle or L. H. mechanism. However, even for the reaction of CO oxidation over copper catalysts, which may be the simplest reaction system, there is still no consensus among researchers because there are many delicate factors that affect the reaction rate (2–4).

Recently, there have been many extensive studies using a single crystal instead of polycrystalline powder to elucidate the surface defects, adsorbed species, and their orientation and active sites (5–8). In order to clarify the relationship between catalytic activity and surface oxidation, Jernigan and Somorjai (9) carried out kinetic measurements of CO conversion to CO_2 over a thin film of copper. They demonstrated that CO oxidation is catalyzed by every oxidation state of copper and that the catalytic activity decreases in the order of $Cu > Cu_2O > CuO$. They also proposed the Langmuir–Hinshelwood model for Cu and Cu_2O and a redox cycle for CuO.

On the other hand, Sadykov and co-worker (2, 10) pointed out the existence of an oxygen defect phase (CuO_x), which occurs as a metastable state and does not determine unequivocally the catalytic activity of the CuO_x phase due to apparent structure sensitivity. It was also pointed out that under mild conditions (below ca 300°C), the catalytic reaction rate depends strongly on the initial oxidation state, while after prolonged treatment at a high temperature (ca. 400–500°C), it is independent of the initial phase differences.

Identification of dioxygen species on the surface of metals and oxides has been an attractive subject because the dioxygen species are the most essential intermediates of many hetrogeneous oxidation reactions (11). One of the powerful techniques for detecting oxygen species is ESR spectroscopy, which is used to resolve adsorbed O_2^- and O^- species. The IR method has been demonstrated to be very useful for determining the oxygen species formed on metals and oxides (12, 13). Adsorbed dioxygens show characteristic frequencies of an O–O bond at around 1500 (O_2), 1100 (O_2^-), and 870 (O_2^-) cm^{-1}, along with the bond orders of 2, 1.5, and 1, respectively (14).

Tanaka *et al.* studied the catalytic oxidation of CO over zinc oxide (15–17) and suggested that the active component is O^-, not O_2^- as was suggested by Morrison *et al.* (18), and that the slow step is the reaction of O^- with weakly adsorbed CO (15, 16). They also indicated that O_2^- on ZnO is inactive for exchange reactions with CO and CO_2 as well as for the catalytic oxidation of CO (17).

Since the concentration of active species may be in a steady state (around zero) in a mixture of CO and O_2, it is
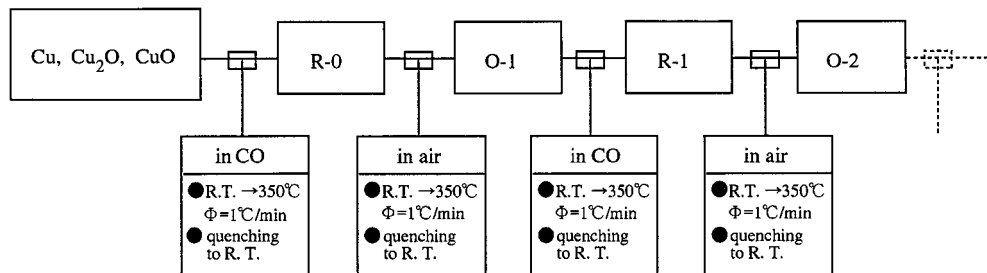
FIG. 1. Flow chart of TG measurement by alternating the reduction process with CO and oxidation process with air.

difficult to discuss dynamics of the catalyst surface only from the data in the gas mixture. Thus, we conducted reactions of the copper oxides with CO and with O_2, individually, and we compared the results with those obtained under conditions in which CO and O_2 coexist, in order to obtain details in the variation in copper valances of a catalyst surface and the roles of adsorbed oxygen species in CO oxidation process on the copper catalysts.

EXPERIMENTAL

Materials

Powdered samples of 99.5% (Cu_2O) and 99.99% (CuO) in purity provided by Wako Pure Chemicals were ground and used as the initial catalysts. Their physical properties are summarized in Table 1.

Apparatus

Thermogravimetric (TG) analysis was performed using a Shinku-Riko MTS-9000 thermobalance with weight sensitivity of 10^{-6} g and a heating rate of $1°C$ min^{-1}, and 40 mg of powdered sample was used for each run. A Rigaku Mini-Flex diffractometer was used for XRD measurements. FT-IR measurements were carried out on a Hitachi DRS-8000 spectrometer with 100 scans at 4 cm^{-1} resolution for the specimens diluted with KBr in a mass ratio of ca. 1/400. In accordance with the program, water vapor and CO_2 adsorption were removed, and smoothing was performed. Specific surface area (*S*) measurements were performed with a Micromeritics Flow Sorb II 2300 apparatus, using the BET method. The electric conductances (EC) were determined by measuring the electric resistance value of the disc sample pressed in vacuum.

Experimental Procedure

The catalytic reactions were studied in a fixed-bed reactor: Streams of 5 vol% CO/He and pure air were fed to 1 g of the catalyst at an equivalent rate of 50 cm^3 min^{-1}. The reactor effluent was analyzed by automatic injection of 1 cm^3 of it into a gas chromatograph equipped with an activated charcoal column.

The reducing process of copper oxide with CO and the reoxidizing process with air (O_2) were monitored by TG according to the scheme shown in Fig. 1. The specimens after quenching to RT were subjected to the appropriate physical measurements.

RESULTS AND DISCUSSION

Catalytic Reactions of CO with Oxygen over Cu_2O and CuO

The temperature-programmed profiles of the CO oxidation over Cu_2O and CuO are shown in Fig. 2, together with those over Cu, CuO*, and no catalyst, where CuO* denotes a Cu(II) oxide after the reaction over Cu_2O. Details of the nature of CuO* are described later. The rate over CuO, which showed almost no change with repeated use,
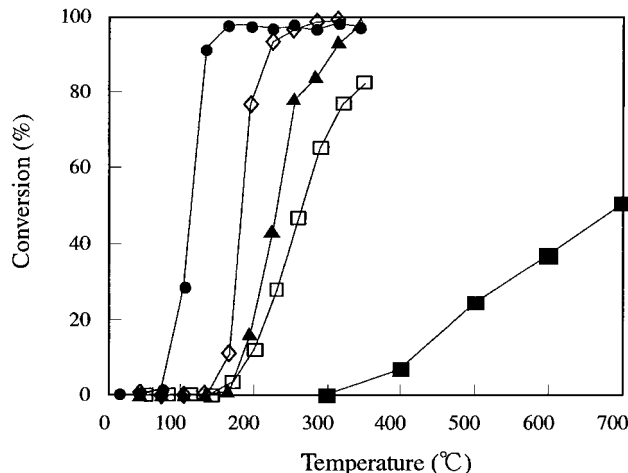

FIG. 2. Temperature-programmed conversion of $2CO + O_2 \rightarrow 2CO_2$ over (▲) Cu_2O, (●) CuO, (◇) Cu, (□) CuO*, and (■) no catalyst.

TABLE 1

Characteristics of Catalysts Used

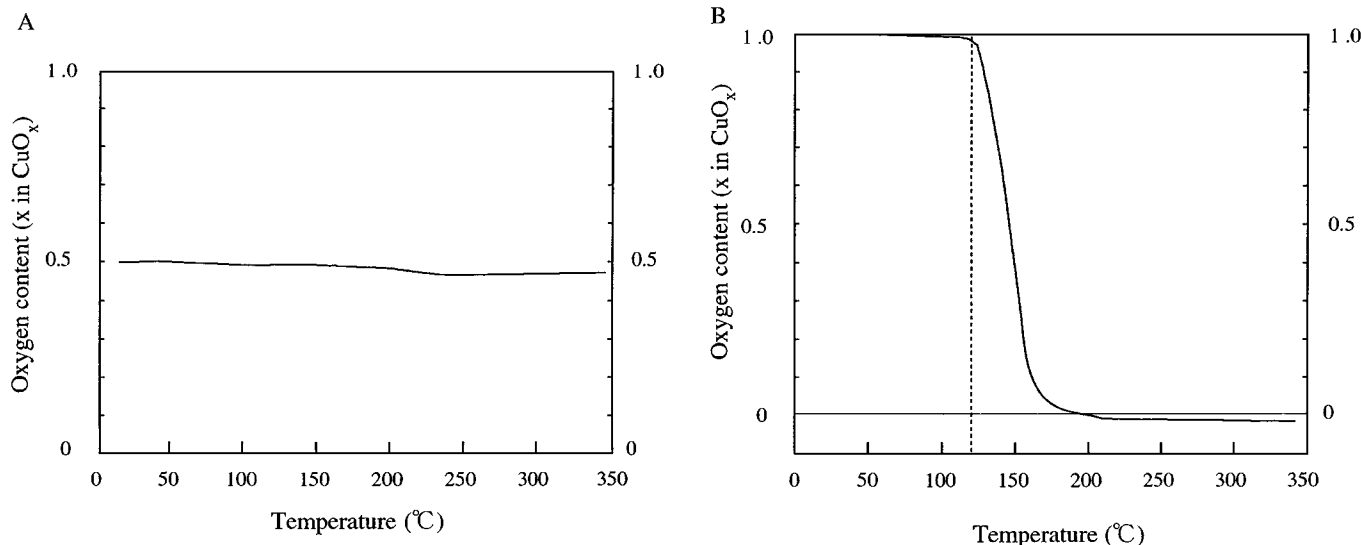| Catalyst	Lattice	IR vibrational frequency ν(Cu–O) (cm^{-1})	ν(O–O) (cm^{-1})	Electric conductivity ($\Omega^{-1} cm^{-1}$)	Surface area $m^2 g^{-1}$
Cu_2O	Cubic	631	1121 (O_2^-)	1.1×10^{-9}	1.1
CuO	Monoclinic	534	1522 (O_2)	1.5×10^{-7}	0.81

A

B

FIG. 3. TG curves of the initial (A) Cu₂O and (B) CuO in 5% CO/He atmosphere, corresponding to each R-0 step.

was much greater than that over Cu₂O (apparently over CuO*), indicating that the surfaces of these oxides were not equilibrated during the reaction.

FT-IR spectra showed the presence of $O_{2\,ads}^{-}$ on the oxide from the initial Cu₂O and the presence of $O_{2\,ads}$ on the oxide from the initial CuO, although both oxides commonly gave an IR band of Cu^{II}–O at around 524 cm^{-1} (CuO*) and 534 cm^{-1} (CuO), respectively. Independent of the initial oxides, postreaction XRD spectra were the same as that of the initial CuO (monoclinic tenorite CuO), indicating that the bulk of the oxides was equilibrated according to the thermodynamical requirement under the gas mixture of CO/O₂ 1/4 in mole ratio (1).

The difference in the adsorbed oxygen species is thought to reflect some important differences in the nature of the surfaces, because formation of $O_{2\,ads}^{-}$ depends on the electron donation ability of the surface and on suitable sites for stabilizing the oxygen species (12). The O₂ adsorption on CuO might seem peculiar, since O₂ is known to adsorb dissociatively on metals and metal oxides, but recent UPS results suggest that $O_{2\,ads}$ on an Mo metal surface is stable up to 500 K and dissociates into atomic oxygen when heated up to 600 K (19).

Oxidizing and Reducing Processes of Bulk Cu₂O

The TG profiles of R-0 and O-1 of Cu₂O are shown in Fig. 3A and Fig. 4A, respectively. These profiles show that the initial Cu₂O can not be reduced by CO but is oxidized by air (O₂) until almost the level of divalent oxide. The formed oxide is by definition CuO*.
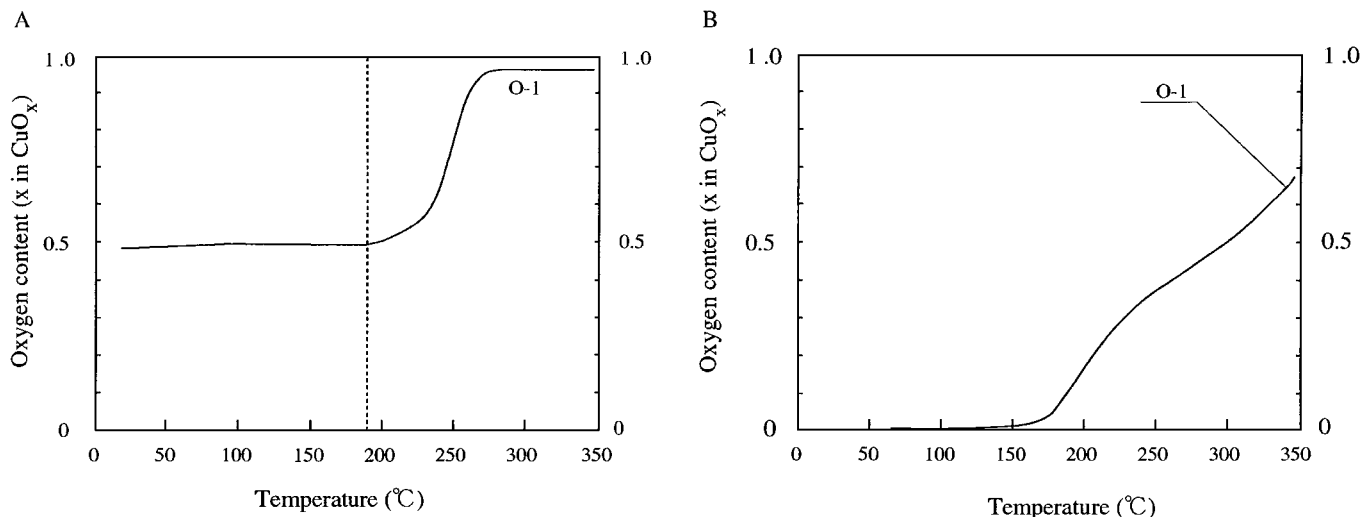
A

B

FIG. 4. TG curves corresponding to each O-1 step of (A) Cu₂O and (B) CuO.

A

B

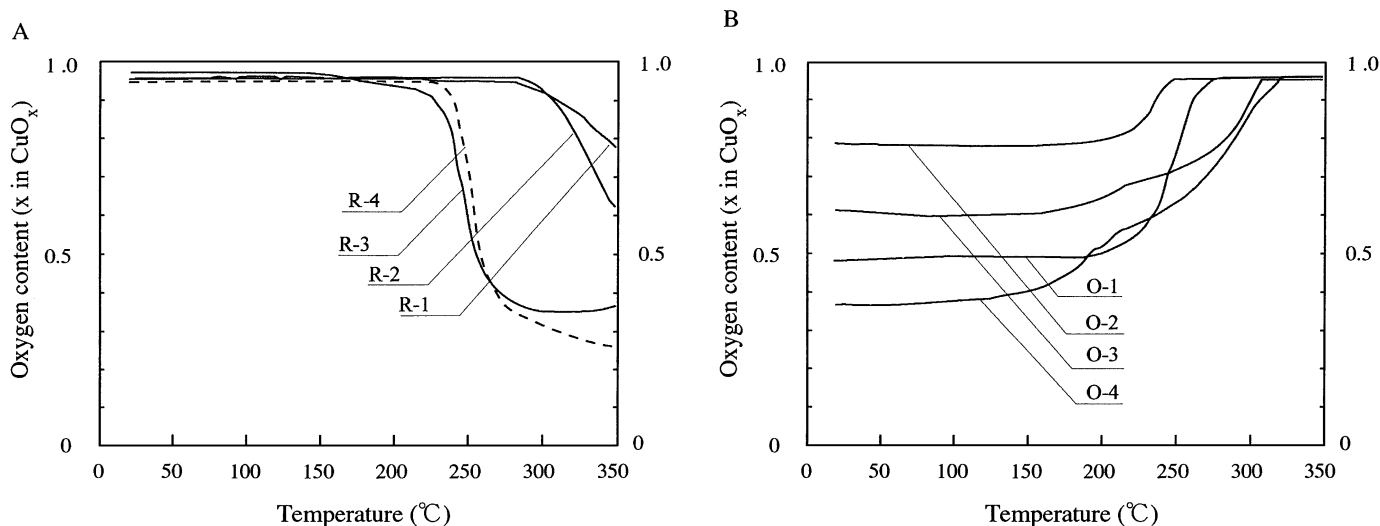**FIG. 5.** TG curves of the alternate (A) reducing and (B) oxidizing processes of Cu_2O.

The TG curves of alternate reducing and oxidizing processes of Cu_2O are shown in Fig. 5. The variations in oxygen content of the products after each process are shown in Fig. 6, and post XRD spectra are shown in Fig. 7, confirming that the copper cycles essentially between Cu(I) and Cu(II) with repetition. It should be noticed that both of the processes shifted to a lower temperature with repetition, reflecting the change in the adsorbed oxygen species O_2^- to O^-, since O_2^- tends to change into O^- at a high temperature and O^- is known to have less resistance to CO reduction than does O_2^- (15). The products of R-1 and R-2 are thought to be Cu_2O, the surface of which is covered by both of O_2^- and O^-, while those of R-3 and R-4 are thought to be Cu_2O, which is covered preferentially by O^-. The products of O-3 and O-4 are thought to be CuO^*, the surface of which is covered by O^- species. The weight loss values given in Fig. 6 suggested that the products of R-3

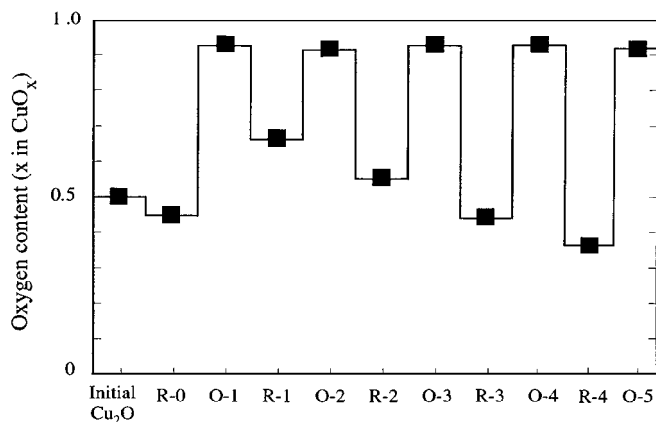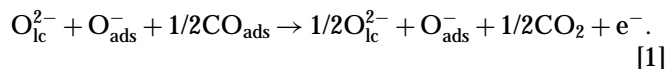and R-4 include Cu metal and that CuO^* includes oxygen defects of ca. 0.05.

It might seem strange that O_2^- $(O^-)_{ads}$ governs the bulk reduction in the absence of free oxygen, if only the following one-way steps were assumed: $O_2 \rightarrow O_2^- \rightarrow O_2^{2-} \rightarrow O^- \rightarrow O_{lc}^{2-}$ (12). Thus, the reverse step of $O_{lc}^{2-} \rightarrow O_{ads}^-$ in the presence of CO was undertaken:

$$O_{lc}^{2-} + O_{ads}^- + 1/2CO_{ads} \rightarrow 1/2O_{lc}^{2-} + O_{ads}^- + 1/2CO_2 + e^-.$$
[1]

Reaction [1] can also explain the observed valence change of Cu^{2+} to Cu^+. The catalytic temperature over Cu_2O was very near the onset temperature of R-3 and R-4 of CuO^*, suggesting that CO oxidation occurs apparently over CuO^*, the surface of which is covered by O^- species.

Reducing and Oxidizing Processes of Bulk CuO

Reduction of the initial CuO into Cu(0) took place at around $120°C$ in one step (Fig. 3B), whereas reoxidation of the formed Cu metal occurred in a stepwise manner (Fig. 4B). As shown in Fig. 8A, there was almost no change in the reduction manner of CuO with repetition. The manner of reoxidation also remained essentially the same with repetition, although the degree of reoxidation of the formed Cu was depressed with repetition owing to considerable sintering of the metal, as shown in Fig. 8B.

The XRD spectra of the products after each process are shown in Fig. 9, confirming the direct reduction from CuO to Cu and the stepwise oxidation of $Cu \rightarrow Cu_2O \rightarrow CuO$. Owing to considerable sintering of the metal, the copper valence appears to settle between 0 and I with repetition, as shown in Fig. 10.

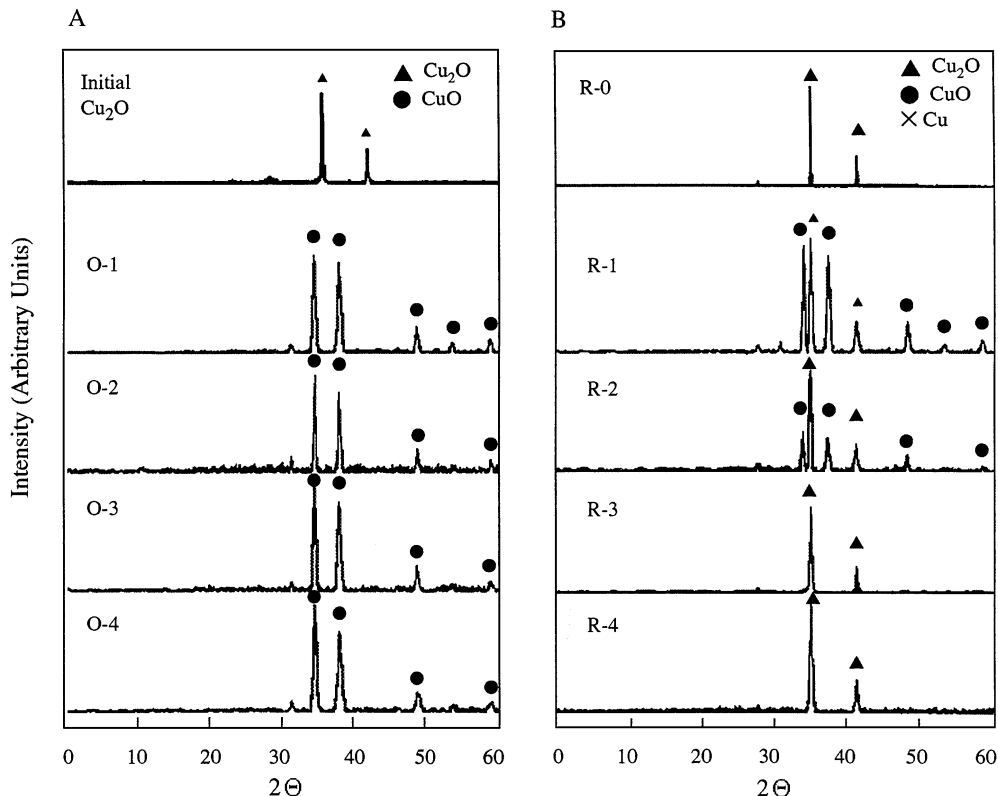It was noticed that Cu_2O from the reoxidation of Cu(0) was easily reduced by CO, indicating that there is a

FIG. 6. Variations in oxygen content evaluated from the TG results in Fig. 5.

FIG. 7. XRD spectra of the products after each (A) oxidizing process and (B) reducing process of Cu$_2$O.

different kind of Cu$_2$O from the initial one. Since the Cu$_2$O from Cu (although it existed always as a mixture of Cu, Cu$_2$O, and CuO during the reoxidizing process) showed IR bands of O$_{2\,ads}$ species at 1503, 1522, and 1578 cm^{-1}, a stoichiometric Cu$_2$O which can be more easily reduced than CuO, is thought to be formed. This obser-

vation is consistent with the previous results using a thin film of copper (9).

The onset temperature of CuO reduction almost agreed with the CO oxidation temperature over CuO. A redox cycle between Cu(II) and Cu(0) on the surface may be appropriate for the catalytic mechanism, and Reaction [2] is a
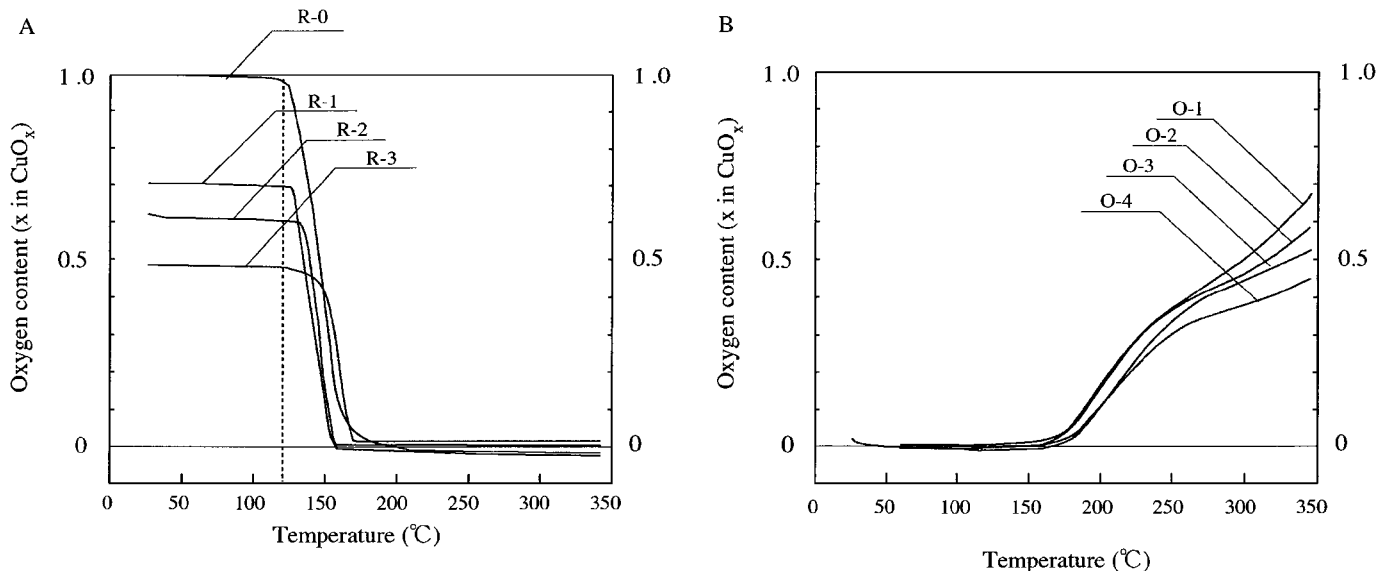

FIG. 8. TG profiles of the alternate (A) reducing and (B) oxidizing processes of CuO.
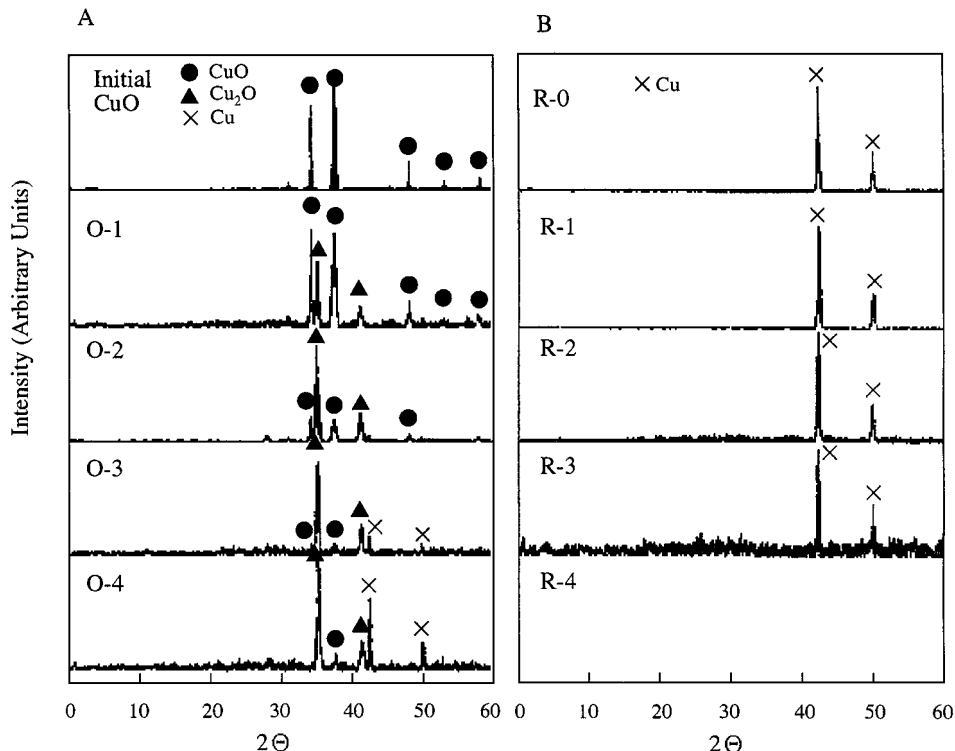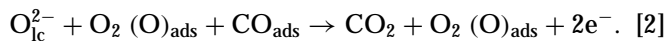
FIG. 9. XRD spectra of the products after each (A) oxidizing process and (B) reducing process of CuO.

possible bulk reaction that can explain the valence change from Cu^{2+} to Cu in the absence of free oxygen.

$$O_{lc}^{2-} + O_2\,(O)_{ads} + CO_{ads} \rightarrow CO_2 + O_2\,(O)_{ads} + 2e^-. \quad [2]$$

Reaction Mechanisms of the Copper Oxides with CO

Surface oxidation of Cu_2O, the surface of which is covered by O_2^-, occurred even at a temperature as low as

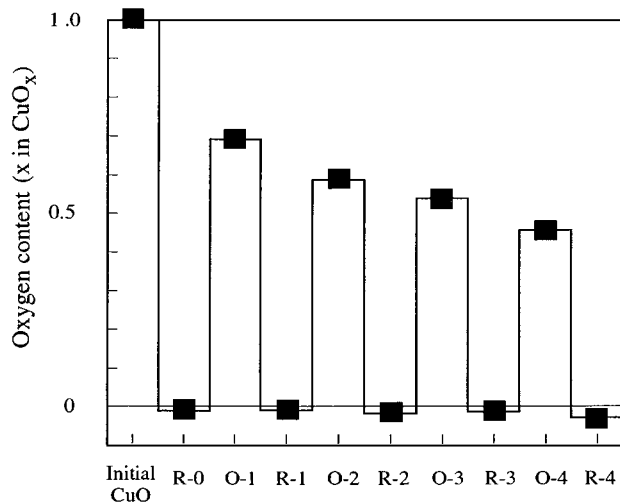**FIG. 10.** Variations in oxygen content of the products with repetition.

$100°C$, judging from the appearance of the Cu^{2+}–O_{lc} band at $518\ cm^{-1}$ (Fig. 11b), and Cu_2O transformed completely into CuO* by heating up to $350°C$ in air (Fig. 11c). Thus, the superoxide species readily allowed O_2 oxidation, compared with the neutral adsorbed species ($O_{2\,ads}$ or O_{ads}). The IR spectra of CuO*, the surface of which is covered by O_2^- and/or O^-, after admission of 5% CO/He at $350°C$ shows IR bands of $CO_{2\,ads}$ at $2350\ cm^{-1}$ (ν_3) (Fig. 11d). Precursors, such as $CuO^* \cdot OCO_{ads}^-$ and/or $CuO^* \cdot O_2CO^-$, may be immediately followed by an electron transfer from the adsorbed species to Cu^{2+} with elimination of CO_2 and reproduction of O_{ads}^- ($O_{2\,ads}^-$).

$$2(CuO^*) \cdot O_{ads}^- + CO \rightarrow 2(CuO^*) \cdot OCO_{ads}^-$$
$$\rightarrow Cu_2O \cdot O_{ads}^- + CO_2. \quad [3]$$
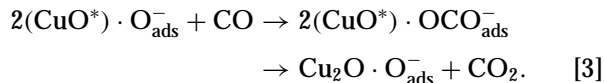
In the case of coexistence of CO and O_2, the oxidation process given by

$$Cu_2O \cdot O_{2\,ads}^- + 1/2O_{2\,ads} \rightarrow 2(CuO^*) \cdot O_{2\,ads}^- \quad [4]$$
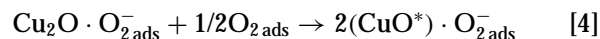
occurred prior to Reaction [5] and was followed by the degradation of O_2^- into O^-.

$$2(CuO^*) \cdot O_{2\,ads}^- \rightarrow 2(CuO^*) \cdot O_{ads}^- + 1/2O_2. \quad [5]$$
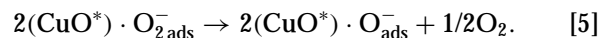
It is known that $O_{2\,ads}^-$ transfers into O_{ads}^- at a high temperature and that O_{ads}^- species can diffuse to bulk by replacing lattice oxygen (20–22).
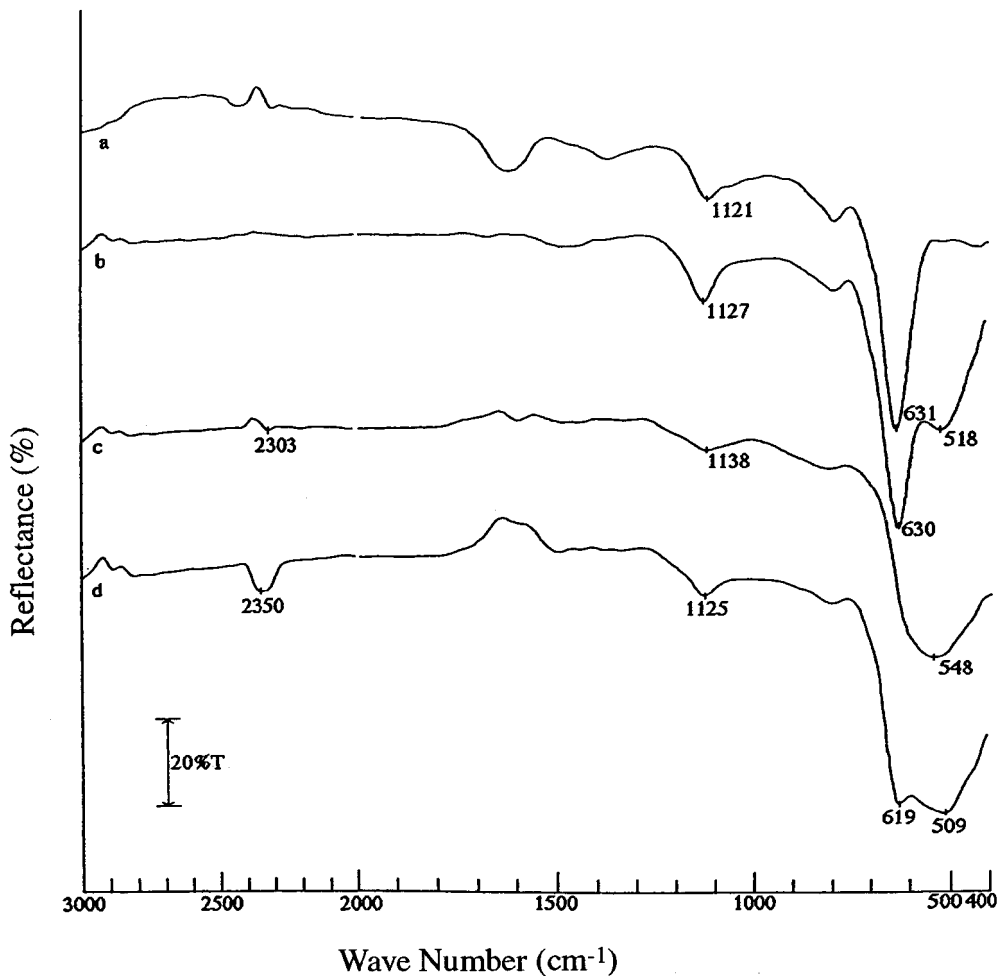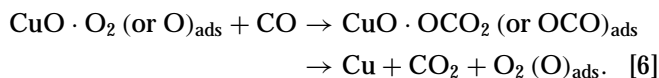
FIG. 11. FT-IR spectra of Cu_2O at RT (a) before and after admission of air (O_2) for 10 min, at (b) 100°C and (c) 350°C. Spectrum (d) corresponds to CuO* after admission of CO for 10 min at 350°C.

Typical FT-IR spectra of CuO before and after admission of air or CO at desired temperatures are shown in Fig. 12. Formation of $O_{2\,ads}$ on CuO was confirmed, judging from the band of $\nu(O-O)$ at around 1500 cm^{-1}. The IR spectrum after admission of CO at 120°C, the temperature that corresponds to the onset of CuO reduction, showed bands of $CO_{2\,ads}$ at 2352 cm^{-1} (ν_3) and 1381 cm^{-1} (ν_1) together with a weak band of CO at 2193 cm^{-1} (Fig. 12c), suggesting the formation of precursors such as $CuO \cdot CO_2$ or $CuO \cdot OCO_2$, which is followed by two-electron transfer from the precursors to Cu^{2+} with elimination of CO_2 and reproduction of $O_{2\,ads}$ or O_{ads} species:

$$CuO \cdot O_2 \ (\text{or } O)_{ads} + CO \rightarrow CuO \cdot OCO_2 \ (\text{or } OCO)_{ads}$$
$$\rightarrow Cu + CO_2 + O_2 \ (O)_{ads}. \quad [6]$$

CONCLUSIONS

It has been shown that the rate of CO oxidation depends only on CO partial pressure (15) when the surface of CuO is almost completely covered by adsorbed oxygen species. The present condition of CO/O_2 1/4 in mole ratio may correspond to such a case. We experimentally confirmed that (i) the rates of CO oxidation were quite different between Cu_2O and CuO even after a steady rate was achieved. (ii) In the cases of both CuO and Cu_2O, there were two phases giving the same XRD spectra but adsorbing different oxygen species. (One is a thermodynamically stable phase and adsorbs neutral dioxygen (O_2) and/or neutral atomic oxygen (O) and the other is a thermodynamically metastable phase and adsorbs anionic dioxygen (O_2^-) and/or anionic atomic oxygen (O^-).) The stable phases of Cu_2O and CuO are thought to have a stoichiometric composition, whereas the metastable phases of Cu_2O (hereafter designated Cu_2O^*) and CuO* are thought to be in an nonstoichiometric state and consequently tend to adsorb oxygen oxidatively). (iii) Cu_2O^* strongly resists CO reduction but readily allows O_2 oxidation to give the metastable phase of CuO*. (iv) $CuO \cdot O_2(O)_{ads}$ was reduced directly to Cu(0) by CO near the catalytic temperature over CuO.
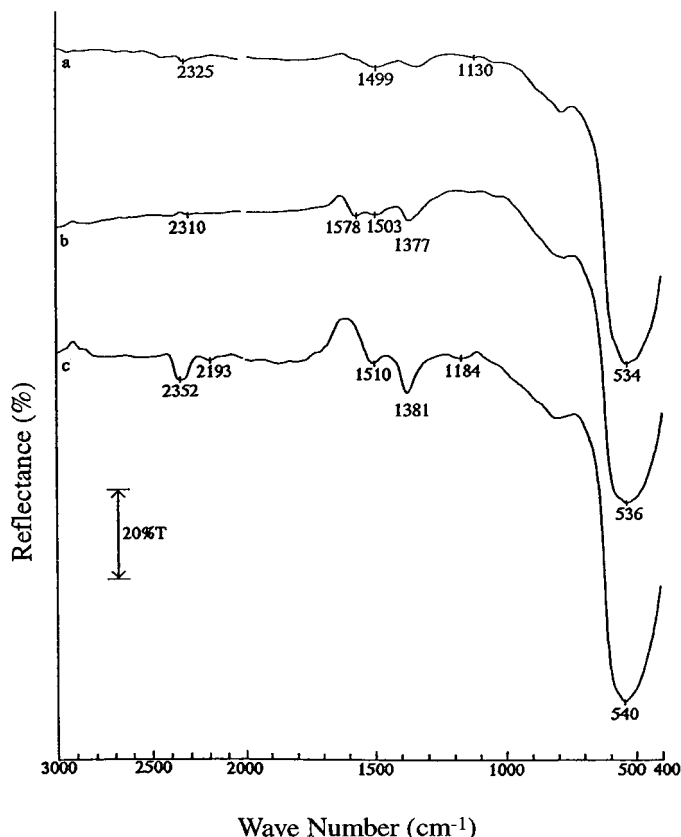
FIG. 12. FT-IR spectra of CuO at RT (a) before and after (b) admission of air at 250°C for 10 min in air and (c) admission of CO at 120°C for 10 min.

(v) $CuO^* \cdot O_{2\,ads}^-$ transformed into $CuO^* \cdot O_{ads}^-$, which was reduced not to Cu(0) but to $Cu_2O^* \cdot O_{ads}^-$ near the catalytic temperature over the initial Cu_2O. (vi) And stoichiometric Cu_2O from the reoxidation of Cu adsorbed O_2 (O) and was easily reduced by CO to Cu metal. From these observations, it can be concluded that when starting from the initial CuO (stoichiometric CuO), copper valence of a catalytic surface cycles between II and 0, and when starting from the initial Cu_2O (nonstoichiometric Cu_2O), copper valence of the surface changes from I to II first and then cycles between II and I during the catalytic process.

REFERENCES

1. O' Keeffe, M., and Moore, W. J., *J. Chem. Phys.* **36**, 3009 (1962).
2. Sadykov, V. A., and Tikhov, S. F., *J. Catal.* **165**, 279 (1997).
3. Choi, K. I., and Vannice, M. A., *J. Catal.* **131**, 22 (1991).
4. Van Dillen, A. J., Geus, J., Geus, J. W., de Jong, K. P., and Van der Meijeden, J., *J. Chem. Phys.* **78**, 979 (1981).
5. Szanyi, J., and Goodman, D. W., *Catal. Lett.* **21**, 165 (1993).
6. Domagla, M. E., and Campbell, C. T., *Catal. Lett.* **9**, 65 (1991).
7. Ertl, G., Hierl, R., Knozinger, H., Thile, N., and Urbach, H. P., *Appl. Surf. Sci.* **5**, 49 (1980).
8. Habraken, F. H. P. M., and Bootsma, G. A., *Surf. Sci.* **87**, 333 (1979).
9. Jernigan, G. G., and Somorjai, G. A., *J. Catal.* **147**, 567 (1994).
10. Kryukova, G. N., Zaikovskii, V. I., Sadykov, V. A., Tikhov, S. F., Popovskii, V. V., and Bulgakov, N. N., *J. Solid State Chem.* **73**, 191 (1988).
11. Vasca, L., *Acc. Chem. Res.* **9**, 175 (1976).
12. Li, C., Domen, K., Maruya, K., and Onishi, T., *J. Am. Chem. Soc.* 7683 (1989).
13. Al-Mashta, F., Sheppard, N., Lorenzelli, V., and Busca, G., *J. Chem. Soc. Faraday Trans. I* **78**, 979 (1982).
14. Nakamoto, K., "Infrared and Raman Spectra of Inorganic and Coordination Compounds," 3rd ed., p. 105. Wiley, New York, 1978.
15. Tanaka, K., and Blyholder, G., *J. Phys. Chem.* **75**, 1807 (1971).
16. Tanaka, K., and Blyholder, G., *J. Phys. Chem.* **76**, 3184 (1972).
17. Tanaka, K., and Miyahara, K., *Chem. Commun.* 877 (1973).
18. Morrison, S. R., and Bonnelle, J. P., *J. Catal.* **25**, 416 (1972).
19. Oknishi, H., Miyachi, M., Fukui, K., Motoda, K., and Iwasawa, Y., *Proc. Catal. Soc. Jpn.* **82A**, 219 (1988).
20. Vayenas, C. G., Bebells, S., and Ladas, S., *Nature* **343**, 625 (1990).
21. Bebellis, S., and Vayenas, C. G., *J. Catal.* 118 (1989).
22. Arakaw, T., Saito, A., and Shiokawa, J., *J. Appl. Surf. Sci.* **16**, 365 (1983).